

**International Journal of
Engineering Research and Science & Technology**



ISSN : 2319-5991

www.ijerst.com

Email: editor@ijerst.com or editor.ijerst@gmail.com

Grid-Integrated PV System with SEPIC Converter Enhanced by Grey Wolf Optimization-Aided MPPT Algorithm

Thati Venkata M. Lakshmi¹, Sri Harsha Giri¹, Apillarisetty Sreya², L.Vijaya Lakshmi², Tallam Sravya Sri², P.Sri Nandu²

¹Assistant Professor, Department of Electrical and Electronics Engineering, SRK Institute of Technology-Enikepadu, Vijayawada-521108, Andhra Pradesh, India

²Department of Electrical and Electronics Engineering, SRK Institute of Technology-Enikepadu, Vijayawada-521108, Andhra Pradesh, India

Abstract:

The current decade has witnessed a significant rise in environmental pollution, escalating fuel expenses, rapid depletion of fossil fuels, and heightened consumer demands. Consequently, this has led to a substantial expansion of Electric Vehicles (EVs). Furthermore, due to the significant pollution emitted by conventional internal combustion engine vehicles, there is a growing demand for electric vehicles powered by renewable energy sources (RES). Of particular importance are electric vehicles (EVs) that rely on photovoltaic (PV) power. These vehicles are highly significant since they can be used all year round and are easy to install. Nevertheless, the sporadic nature of photovoltaic (PV) systems results in voltage swings. Hence, it is imperative to enhance the productivity of the photovoltaic (PV) system. This study utilizes an enhanced DC-DC SEPIC converter to boost the output of a photovoltaic (PV) system, which is then applied in electric vehicle (EV) applications. A closed loop technique based on Grey Wolf Optimization (GWO) is employed to ensure a constant DC link voltage at the output of the DC-DC converter. Additionally, the SEPIC converter's output is sent to the Voltage Source Inverter (VSI), where it is transformed into an AC power supply and then supplied to the electric vehicle (EV) or grid. The process of achieving grid synchronization is facilitated by the utilization of a PI controller. The proposed work aims to minimize total harmonic distortion (THD) and decrease switching losses, leading to improved energy management in electric vehicles (EVs) and ensuring uninterrupted power supply. In addition, to assess the effectiveness of the suggested methodology, it is implemented using MATLAB/Simulink.

Key Words: Electric Vehicles (EVs), Renewable energy sources (RES), Single ended primary inductance converter (SEPIC), Grey Wolf Optimization (GWO), Voltage source inverter (VSI) and Total harmonic distortion (THD).

1. INTRODUCTION:

Energy shortages and rising energy worries have risen dramatically in recent decades, prompting the development of potential new approaches including renewable power production and the electrification of transportation. Statistical analysis reveals that over 90% of passenger cars are parked for longer periods of time than it takes for their batteries to fully recharge. Electric cars (EVs) are better for the environment than conventional vehicles powered by internal combustion engines[1], and Plug-in Electric Vehicles (PEVs) powered by batteries provide an efficient alternative source. In 2016, there were 2.3 million charging stations for EVs, most of which are linked to the grid [2]. However, RES-based EVs are recommended in order to achieve the fundamental benefits of Electric Vehicles (EVs), such as

reduced pollution, decreased fossil fuel reliance, and increased energy security. Although other renewable energy sources (RES) including solar, wind, and tidal are all viable options, a solar-powered EV charging station is the most convenient option. All of the charging stations likely use DC-DC converters to link the PV array to the station [2]. Variations in power transmission between the PV system and the grid occur often due to the intermittent nature of solar irradiation. In order to increase the PV system's output voltage, a DC-DC boost converter is required, since it not only offers greater efficiency and gain, but is also a vital component of the system [3]. Buck-Boost converters (BBCs) are basic converters used to boost voltage gains by boosting or dropping the source voltage within a narrow range.

In addition, the switch's duty ratio determines whether the BBC operates in step-up or step-down mode. The BBC works in step-up mode when the duty ratio is more than 0.5, and in step-down mode when it is less than 0.5. There are several negative aspects of the BBC, such as its inverting output, high voltage stress, and low voltage gain. The voltage gain of the BBC converter may be increased by the use of a high duty cycle [4, 5]. Furthermore, DC-DC Cuk converters are favoured due to its ability to achieve continuous output and input current in addition to minimised output voltage ripples. There are three distinct modes of operation for this converter design: "buck," "boost," and "buck-boost." All three modes work on the same basic idea to provide different voltages and help increase the input voltage. To add insult to injury, being a fourth-order system [6, 7] means that the Cuk converter produces a negative output voltage. Reduced switching losses and conduction due to reduced switch current stress are two of the benefits provided by a switched inductor Cuk converter for EV applications in [8]. Since inductance is already present at the converter's input, problems with peaky current are completely ruled out. However, it is only appropriate for uses that call for power with high current and low output voltage, therefore it won't help with narrow input voltage concerns. In addition, the non-linear behaviour of the system is a result of the switching between DC-DC converters. The converter's non-linear diode and transistor models have capacitive effects, which cause sub-harmonic oscillations [9].

When a tiny film capacitor [10, 11] is used in lieu of the electrolytic capacitor typically used in DC-DC Cuk converters, the converter's lifespan is extended, but the link capacitor voltage is not constrained to remain within the positive range and may even drop below zero. Switched inductor technology in Cuk converters allows for higher static gain and lower switch voltage. Soft switching approaches, however, allow for much greater gains in converter efficiency. One major problem, however, is that the converter's output has the wrong polarity. As a result of the converter's harsh switching circumstances, power conversion efficiency decreases, which is the next disadvantage. A DC-DC converter called a Single ended primary inductor converter (SEPIC) is used to address these concerns since it results in lower ripples at the converter's terminals. The SEPIC converter is used in PV applications due to its versatility in connecting to a wide range of PV modules and batteries, and its flexibility to step up or down the voltages being converted. In addition, the SEPIC converter has the same capabilities as the Cuk converter, other from the fact that the polarity of the output voltage is flipped. SEPIC converter has a significant impact on power conversion and is used in a broad variety of industrial settings due to its advantageous properties [12, 13].

The input impedance of a SEPIC converter may be modified by adjusting the duty cycle.

Because of its stable voltage and current output, it is an excellent choice for uses requiring such parameters. The SEPIC converter is favoured in PV systems because of this quality. At addition, the input current ripples are less because of the inductor in the front end [14]. However, the controller design of a SEPIC converter is challenging since it is non-linear and a fourth order converter. Additionally, SEPIC converter behaviour is affected by load changes and operating circumstances [15]. To address these challenges, the proposed study introduces a redesigned SEPIC converter for usage in PV fed grid connected Electric car applications. The proposed work makes use of a new and better SEPIC converter to increase the PV system's output, and it uses a Grey Wolf Optimization based closed loop approach to keep the SEPIC converter's DC-link voltage stable. The achieved DC-link voltage is then

either sent into the grid or the EV's battery. Grid synchronisation is achieved with the use of a PI controller. The suggested work provides an uninterrupted flow of power to the car at all times.

II. PROPOSED SYSTEM

In light of the limited availability of fossil fuels, renewable energy sources and the RES based EV applications have received considerable focus. Solar, wind, tidal, etc. are some of the most widely used RES, and PV-based EVs have gained significant ground in recent years. The PV system provides emission-free power, is simple to set up, and is always in operation. However, the output of PV systems varies from time to time due to the frequent changes in solar irradiation. In addition, maintaining a steady rate of output from the PV system becomes increasingly challenging. Because of this, the proposed work uses a novel DC-DC improved DC-DC SEPIC converter for EV applications.

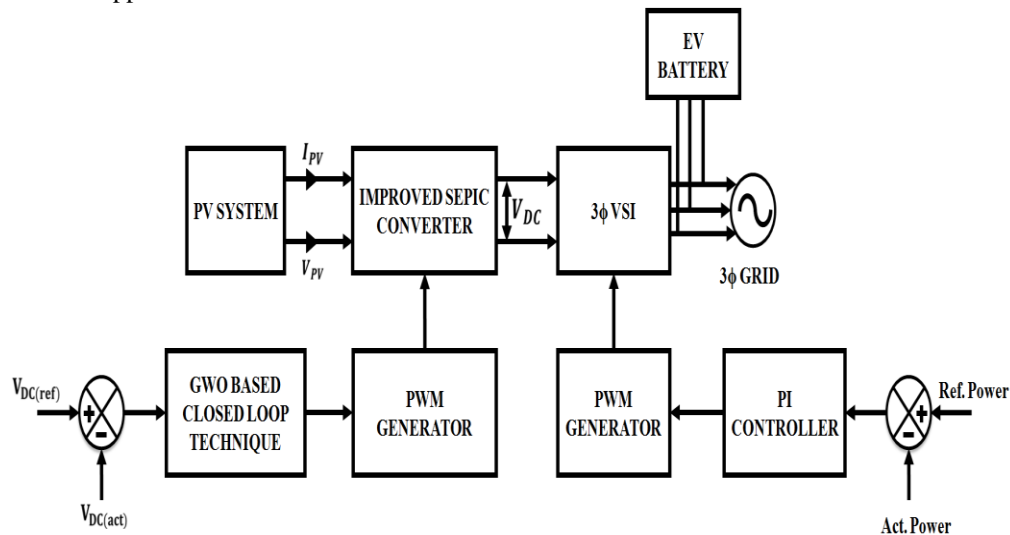


Figure 1 Block diagram of the proposed system

Pictured in Figure 1 is the proposed block diagram. When used in conjunction with a Grey Wolf Optimization based closed loop technique, a SEPIC converter can improve the PV system's output even as its output voltage varies, and it can help keep the DC-link voltage stable. Next, it goes to the SEPIC converter via a pulse width modulation (PWM) generator. In addition, a VSI is used to transfer the DC-link voltage from the output to either the grid or the EV. A PI controller is used to synchronise the grid, which in turn lowers the THD.

2.1 PV system Modelling

The PV system is the primary contributor to electricity production since it is a major renewable energy source. Solar photovoltaic (PV) systems rely mostly on semiconductor diodes that are directly exposed to sunlight. Several photons from the solar irradiance are absorbed by the p-n junction, and their energies range from very low to very high. The energy created by photons with an increased amount of energy over the band gap is used at a level corresponding to the band gap, while the excess energy is dissipated as heat. The equivalent circuit of a PV system is shown in Figure 2, where r_s and r_p stand for the resistances in parallel and series, respectively. Since the value of r_s is rather little while the value of r_p is quite large, it is convenient to ignore both of them in this case.

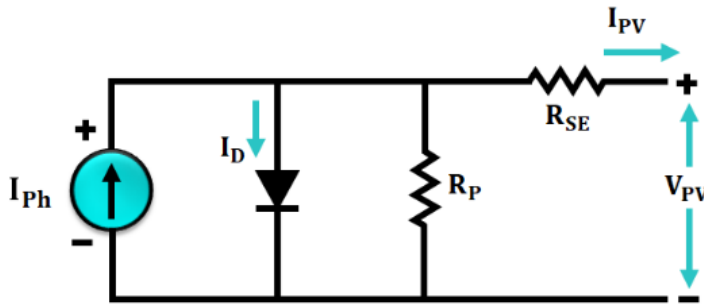


Figure 2 Equivalent circuit of photovoltaic system

The estimation of the VI characteristics of the PV system is given as follows. The representation of photo-current in the PV system is,

$$I_{pc} = [I_{si} + K_i(T - T_o)] * \frac{G}{100} \tag{1}$$

Photo-current is denoted by, short-circuit temperature by, operating temperature by T in Kelvin, the reference temperature by, and solar irradiation by G in (Typically, PV cells are connected in groups known as PV modules, and these modules are connected either in parallel or series with the PV system. Saturation current in the opposite direction for a module is represented as,

$$I_r = \left[\frac{I_{si}}{\exp\left(\frac{qV_o}{N_s K n T}\right) - 1} \right] \tag{2}$$

In the above equation, the reverse saturation current is denotes as I_r , short circuit current is represented by I_{si} , q is denoted as charge of the electron, open circuit voltage is given by V_o , total number of PV cells that are connected in series are denoted by N_s , ideality factor of the diode is denoted by n and the Boltzmann constant is represented as K . The output current of the PV system is expressed as,

$$I_{PV} = N_p * I_{pc} - N_p * I_s * \left[\exp\left(\frac{V_{PV} + I_{PV} * \frac{R_s}{N_p}}{n * V_{th}}\right) - 1 \right] - I_p \tag{3}$$

Here, the number of cells connected in parallel is denoted as N_p , saturation current is denoted as I_s , output voltage is denoted as V_{PV} , the diode thermal voltage is represented by V_{th} and the parallel current is given by I_p . From the values of Boltzmann constant, the V_{th} is computed, while the parallel current, electron charge and operating temperature is obtained from the number of cells linked in parallel and series, also from the parallel and series resistance. Further, the output power achieved from system is fed to the improved SEPIC converter.

2.3 Modelling of Improved SEPIC converter

The Improved SEPIC converter takes the output of PV system as its input. Since the conventional SEPIC converter possess the step-up and step-down static gain operating characteristics, it is highly employed in wide input voltage applications. Nevertheless, sum of output and input voltage is equivalent to the switch voltage, due to which there is reduced static gain than the classical boost converter. This issue is eliminated by introducing a novel SEPIC converter that involves an additional capacitor C_M and a diode D_M , which is illustrated in Figure 3.

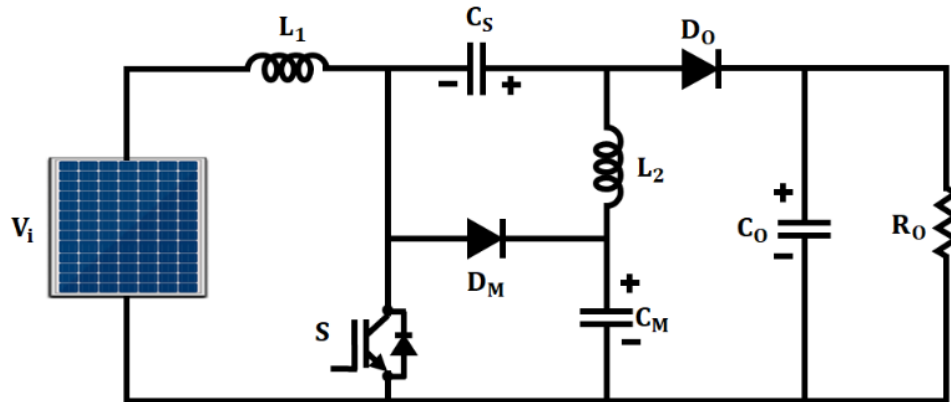
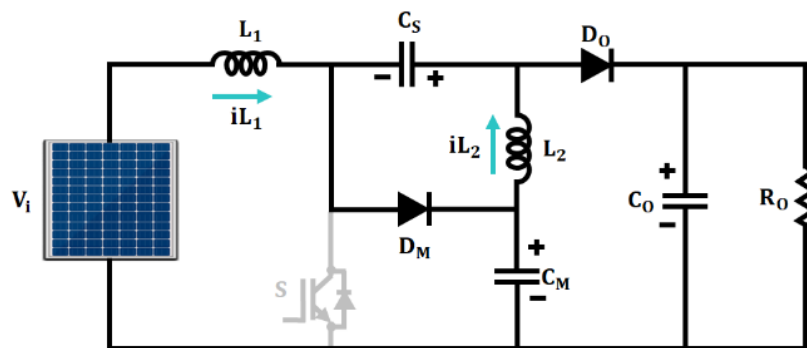


Figure 3 Equivalent circuit of Improved SEPIC converter

Different values of converter static gain result in a wide range of operational characteristics for the proposed improved SEPIC converter. The continuous conduction mode of the enhanced SEPIC converter involves two distinct operating modes. In a purely theoretical analysis, semiconductors would be idealised while capacitors would serve as voltage sources. This revised SEPIC converter has two modes of operation, which are as follows.

Mode 1 [$t_0 - t_1$]: In the first stage, the switch S is in OFF condition at a time instant of t_0 and through C_s and D_s the energy stored in the inductor L_1 is shifted to the output. It is also transferred to the C_M via D_0 . Therefore, the C_M becomes equivalent to the switch voltage. Further, with the aid of D_0 , the energy stored in L_2 , is moved to the output.

Mode 2 [$t_1 - t_2$]: In the second stage, the switch S is in ON condition, inductors L_1 and L_2 stores energy, also the diodes D_1 and D_2 gets blocked. During this stage, the L_1 is fed with the input voltage and the L_2 is fed with voltages $V_{CS} - V_{CM}$. Moreover, the V_{CM} is greater than the voltage V_{CS} .



(a)

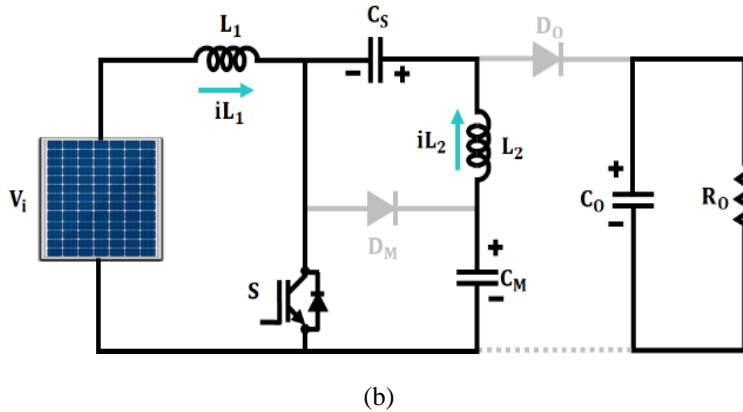


Figure 4 Stage 1 and Stage 2 of Improved SEPIC converter

In consideration with the static gain, the achieved static gain with the aid of the defined converter is greater than the classical boost converter and the nominal duty cycle of the converter is expressed as,

$$D = \frac{V_o - V_i}{V_o + V_i} \quad (4)$$

The voltage at C_M is equivalent to the maximum voltage of all diodes and power switch, also the sum of voltages at C_M and C_S is equal to the output voltage. Assuming that the capacitor voltage ripple ΔV_C is equivalent to nominal voltage of C_M , the capacitance is computed as,

$$C_S = C_M = \frac{I_o}{\Delta V_C \cdot f} \quad (5)$$

Furthermore, the average inductance L_2 and L_1 current is equal to output and input current and is expressed as,

$$L_1 = L_2 = \frac{V_i - D}{\Delta i_L \cdot f} \quad (6)$$

The voltage across the diode and the switch voltage is equivalent to the voltage at the capacitor C_M and is given by,

$$V_S = V_{D0} = V_o - V_M = \frac{V_i}{1 - D} \quad (7)$$

In the proposed work, the improved SEPIC converter attains the output from the PV system and boosts it to the required level. In order to maintain constant DC-link voltage at the output of the SEPIC converter, it is fed to a GWO based closed loop technique with PI controller.

2.4 Modelling of GWO based closed loop technique

2.4.1 Modelling of PI controller

A PI controller is used to regulate the SEPIC converter's output DC-link voltage. The error signal is calculated by the PI controller by comparing the actual output to the target value. The error is calculated by deducting the achieved actual output from the reference value. Subtracting from or adding to the inputs further reduces the error, bringing the process variable close to the set point. This method is typically used in situations

where a complex mathematical model is required. The PI controller output in time domain is measured by the feedback error and the expression for it is given as follows,

$$u(t) = K_p e(t) + K_i \int e(t) dt \quad (8)$$

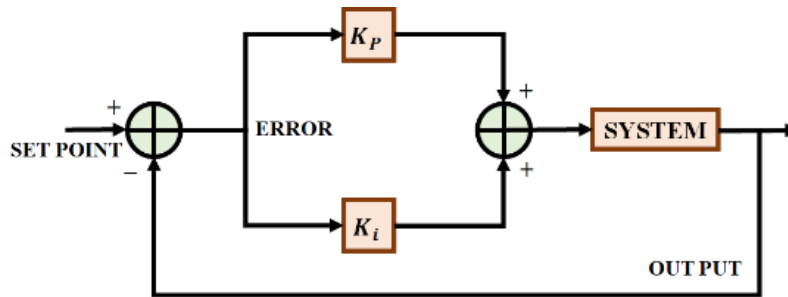


Figure 5 Closed loop PI controller

Here, e is tracking error and is the difference amid actual and the expected performance. On application of Laplace transform on either sides of the above equation, we get,

$$U(S) = \left(K_p + \frac{K_i}{S} \right) E(S)$$

$$\frac{U(S)}{E(S)} = K_p + \frac{K_i}{S} \quad (9)$$

Since, PI controller is associated with improved SEPIC converter, the steady state error is highly decreased and makes the system, a stable one without any fluctuations. In order to fine tune the control parameters of the PI controller, Grey Wolf optimization technique is employed.

2.4.2 Grey Wolf Optimization (GWO)

The GWO algorithm takes its cues from the hunting and pack-leading techniques of Grey wolves, making it a naturally-inspired algorithm. The grey wolf is at the top of the food chain and lives in packs. Alpha, beta, delta, and omega grey wolves are used to model different tiers of authority in a pack. When creating a mathematical model of the wolf pack's social structure, alpha wolves are assumed to be the healthiest and most successful option. Further, beta and delta wolves are considered to be the best alternatives. The final group of potential answers is taken as omega. Hunting, pursuing, tracking, and attacking prey are all part of the GWO algorithm. These steps are useful for developing the GWO algorithm's structure. Examples of grey wolves' circling behaviour include,

$$D = C \cdot X_p(t) - X_p(T) \quad (10)$$

$$X(t + 1) = X_p(t) - A \cdot D \quad (11)$$

Here, the current iteration is given by t , coefficient vectors are represented as D , A and C , position vector of prey is denoted by X_p , position vector of grey wolf is given by X . The value of A and C are computed as follows.

$$A = 2a \cdot r1 - a \quad (12)$$

$$C = 2 \cdot r2 \quad (13)$$

Iteration by iteration, the value of a decreases linearly between 2 and 0, and r_1 and r_2 represent random vectors between 0 and 1. Optimizing the solution can be done by tweaking the values of A and C vectors. The grey wolf adjusts its location using the random vectors r_1 and r_2 . The GWO also aids in maintaining a constant DC-link voltage in the defined work, from the current DC-link voltage (represented by the actual wolf position) to the best wolf position (representing the optimal voltage). Therefore, the PI controller's parameters are adjusted with the GWO algorithm so that the resulting DC-link voltage is optimal. An improved SEPIC converter receives the reference signal at its output from the PI controller via a pulse width modulation (PWM) generator, which compares the reference signal to the carrier signal and generates the corresponding pulses for the SEPIC converter's switches, thereby keeping the DC-link voltage at the converter's output stable.

2.5 Three phase Voltage source inverter (VSI)

An upgraded SEPIC converter's output is fed into the grid via a voltage source inverter. The term "Inverter" is used to describe the converter that changes the DC supply into the AC supply. A three-phase Voltage source inverter converts the direct current (DC) source into alternating current (AC). The six switches that make up a 3 VSI, numbered S1 through S6, work in tandem with one another as follows: S1 and S4, S2 and S5, and S3 and S6.

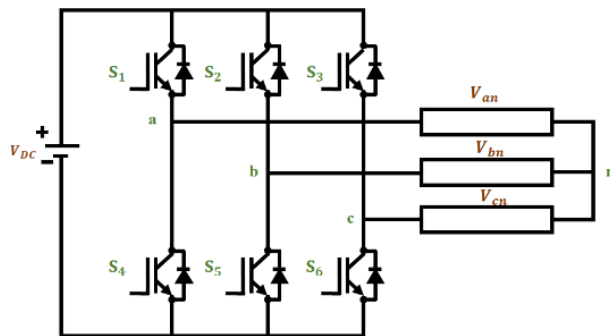


Figure 6 Circuit diagram of 3 ϕ VSI

Circuit diagram of three phase VSI is shown in Figure 6. In the defined work, the output of the SEPIC converter is converted into AC supply using VSI, and then it is delivered to the grid after achieving grid synchronisation using the PI controller. The power is also useful for recharging the electric car's battery. The planned improvement ensures the EV has a constant, uninterrupted source of electricity. In the event of grid failure, PV backs up the EV, and vice versa if there is a shortage of PV power. As a result, the EV has superior energy management thanks to its uninterruptible power supply, and the defined work provides low THD and reduced switching losses.

III. RESULTS AND DISCUSSION

Because of its substantial nature, PV systems are well-suited for EV applications, and the intermittent nature of PV systems is overcome by using an enhanced SEPIC DC-DC converter. To keep the DC-DC converter's output voltage stable, a GWO-assisted PI controller is used. The output of the SEPIC converter is fed to the grid via VSI once grid synchronisation has been achieved. This work brings efficient energy management, making it a good fit for EV applications. In addition, MATLAB/Simulink is used to probe the defined work's efficiency. Table 1 details the project's requirements..

Table 1 Proposed work specifications

	Parameters	Ratings
Solar Panel	Temperature range	-40 to 85°C
	Operating current	5.8A
	Operating voltage	16.8V
	Maximum voltage	1000V DC
	Number of panels	10
	Total number of series cells	36
	Cell area	125mm×31.25mm
Converter	Switching frequency	10Khz
	Capacitors C_1, C_2 & C_M	47μF, 47μF and 100μF
	Inductors L1 & L2	60mH
	Diode D_0 & D_M	MUR 1560

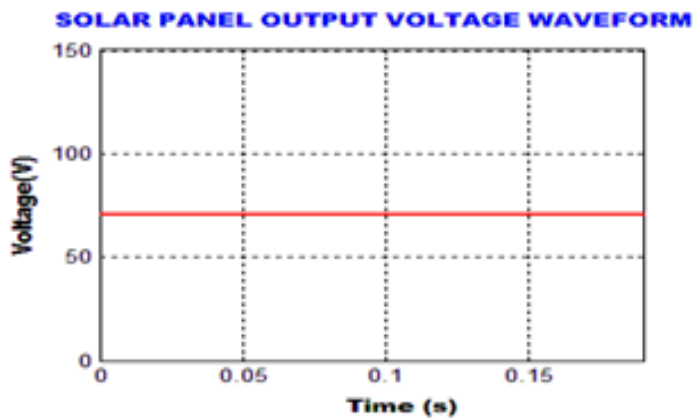


Figure 7 Output voltage waveform of PV system

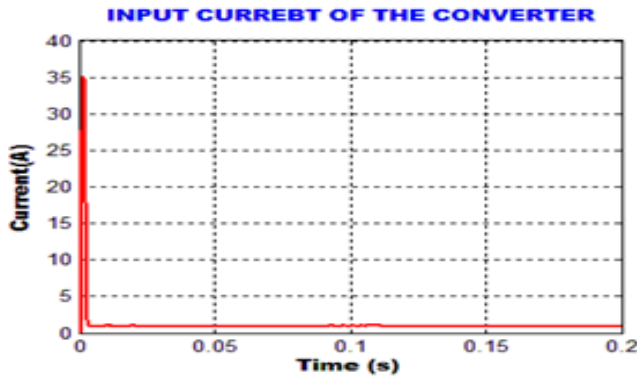


Figure 8 Input current waveform of the converter

The output from the PV panel is around 70V, which is fed as input to the improved SEPIC converter. Figure 7 and Figure 8 illustrates the output voltage and current waveforms of the Solar panel.

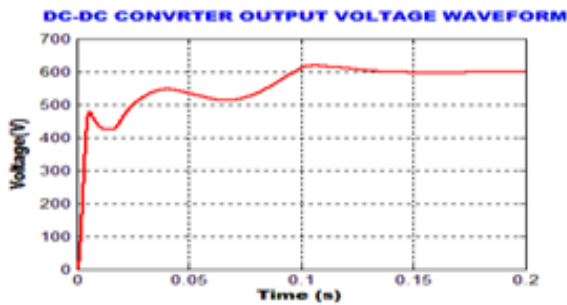


Figure 9 Output voltage waveform of Improved SEPIC converter

The DC output from the PV panel is boosted from 70V to the required level of about 600V. Figure 9 and Figure 10 illustrates the output voltage and current waveforms of the DC-DC improved SEPIC converter.

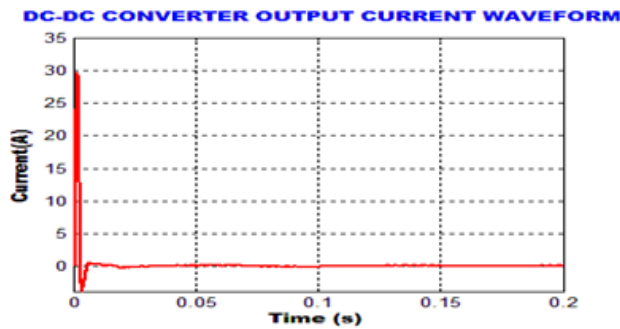


Figure 10 Output current waveform of Improved SEPIC converter

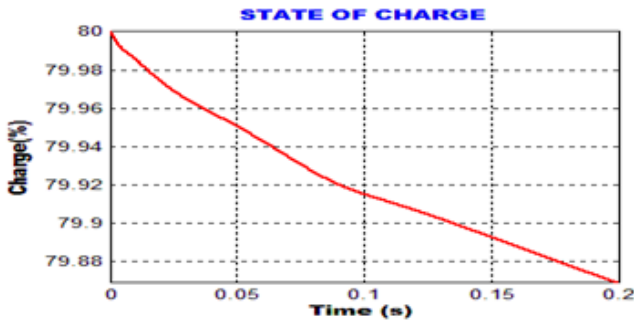


Figure 11 SOC of the battery

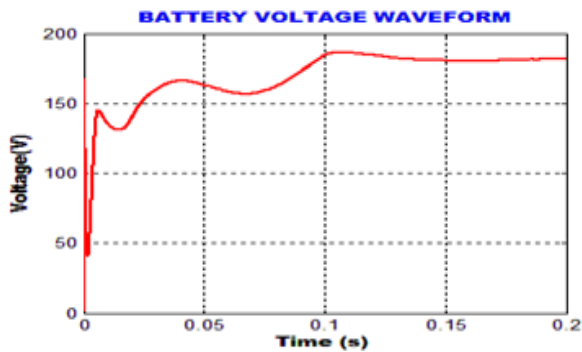


Figure 12 Voltage waveform of the Battery

The SEPIC converter's output is then supplied to either the grid or the EV via a voltage source inverter. The battery charge status of the electric vehicle is shown in Figure 11. The state of charge (SOC) of the battery is used for energy management. The battery's state-of-charge (SoC), which is depicted in Figure 11, provides an indication of the battery's total energy capacity. After a 0.1s time interval, as shown in Figure 12, the battery voltage waveform is stable at around 175V. The battery's current waveform is depicted in Figure 13; it exhibits an initial peak and subsequent decline over the course of about 0.1s.

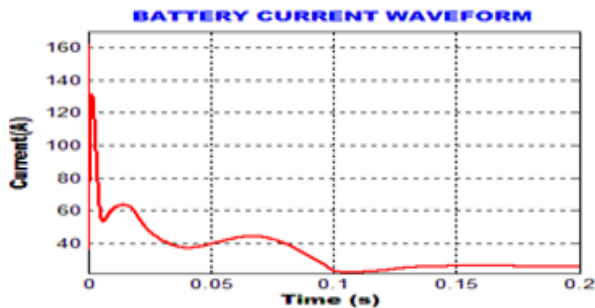


Figure 13 Current waveform of the Battery

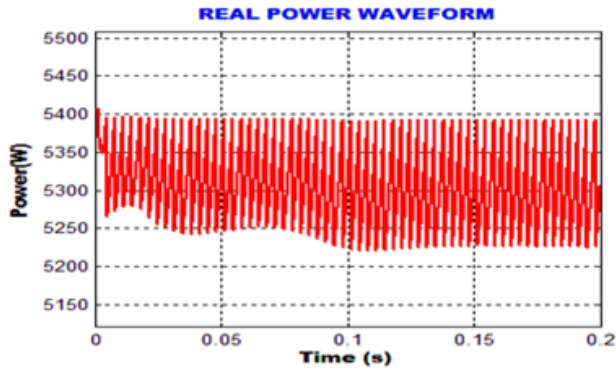


Figure 14 Real power waveform

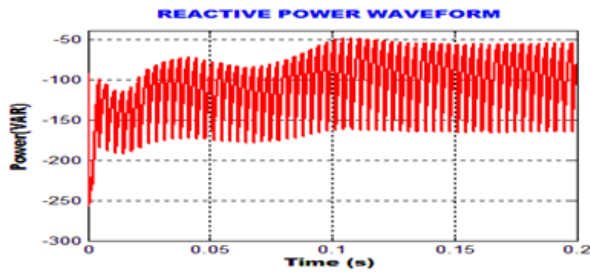


Figure 15 Reactive power waveform

Figure 14 shows the real power waveform, in which the power is maintained constant at about 5395W and Figure 15 shows the reactive power waveform.

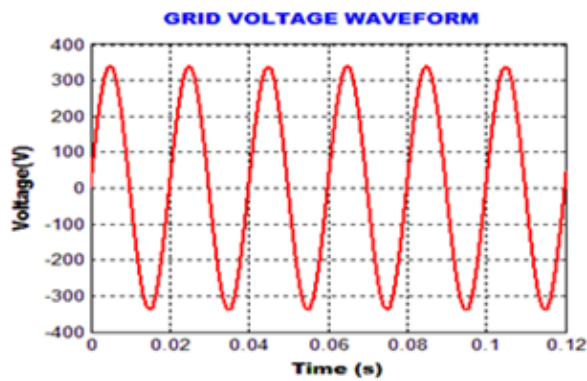


Figure 16 Grid voltage waveform

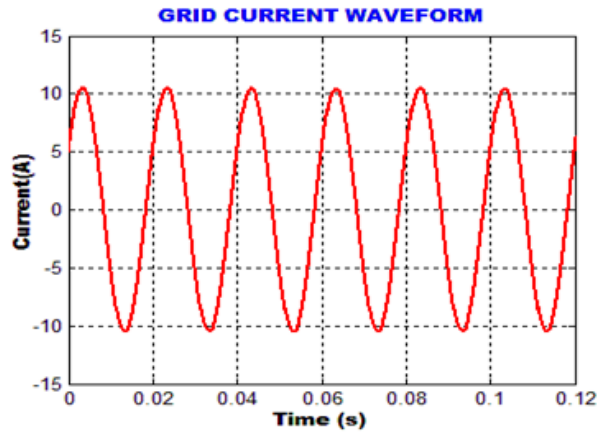


Figure 17 Grid Current waveform

Figure 16 illustrates the grid voltage waveform and is about 320V, while Figure 17 shows the grid current waveform, which is maintained at about 10A. By attaining grid synchronization with the aid of a PI controller, the output from the VSI is fed to the grid.

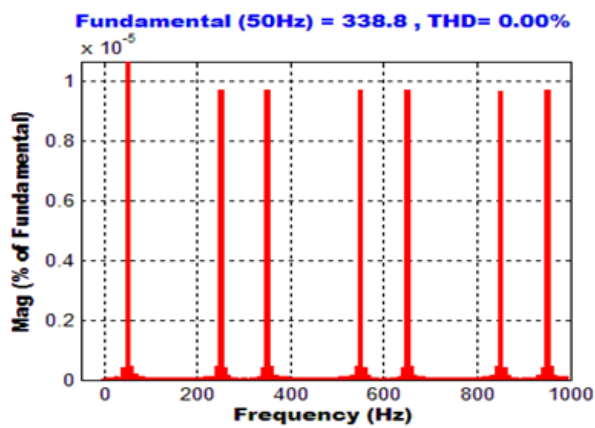


Figure 18 Waveform of Grid voltage THD

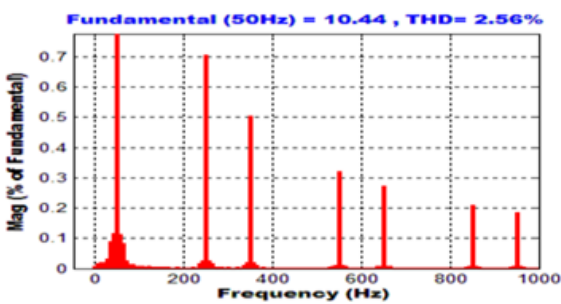


Figure 19 Waveform of Grid Current THD

The proposed work contributes to superior THD reduction, stress-free switching, reactive power compensation, and impressive gains. Grid current waveforms and voltage total harmonic distortion (THD) waveforms are depicted in Figure 18 and Figure 19, respectively. Current THD of 2.56% is quite good when compared to other approaches. One more advantage of the defined work is improved energy management in electric vehicles (EVs) that do not experience power outages.

IV. CONCLUSION

Researchers pay a lot of attention to PV systems because of their low environmental impact and simple set up. Maybe it's not possible to get a constant power supply from the PV system because solar irradiation is always changing. Thus, in this paper, we use a revised SEPIC converter to boost the PV system's output. In addition, the DC-link voltage at the SEPIC converter's output is kept stable with the help of a GWO assisted closed loop technique. The DC from the SEPIC converter is then applied to the grid or EV via a VSI. As a result of the proposed work, electric vehicles will be able to better manage their energy consumption. The EV is able to get its power from both the PV system and the grid. In the event of a failure in either source, the EV system can continue to operate on power from the other. The proposed work is implemented in MATLAB/Simulink so that its performance can be studied. As a result, the proposed work reduces total harmonic distortion (THD) and significantly improves energy management in EV.

REFERENCES

- [1] Q. Yan, B. Zhang and M. Kezunovic, "Optimized Operational Cost Reduction for an EV Charging Station Integrated With Battery Energy Storage and PV Generation," *IEEE Transactions on Smart Grid*, vol. 10, no. 2, pp. 2096-2106, (2019).
- [2] A. Verma and B. Singh, "Multimode Operation of Solar PV Array, Grid, Battery and Diesel Generator Set Based EV Charging Station," *IEEE Transactions on Industry Applications*, vol. 56, no. 5, pp. 5330-5339, (2020).
- [3] M. Arjun, V. V. Ramana, R. Viswadev and B. Venkatesaperumal, "Small Signal Model for PV Fed Boost Converter in Continuous and Discontinuous Conduction Modes," *IEEE Transactions on Circuits and Systems II: Express Briefs*, vol. 66, no. 7, pp. 1192-1196, (2019).
- [4] N. Rana and S. Banerjee, "Development of an Improved Input-Parallel Output-Series Buck-Boost Converter and Its Closed-Loop Control," *IEEE Transactions on Industrial Electronics*, vol. 67, no. 8, pp. 6428-6438, (2020).
- [5] H. S. Son, J. K. Kim, J. B. Lee, S. S. Moon, J. H. Park and S. H. Lee, "A New Buck-Boost Converter With Low-Voltage Stress and Reduced Conducting Components," *IEEE Transactions on Industrial Electronics*, vol. 64, no. 9, pp. 7030-7038, (2017).
- [6] W. Chen, Y. Liu, X. Li, T. Shi and C. Xia, "A Novel Method of Reducing Commutation Torque Ripple for Brushless DC Motor Based on Cuk Converter," *IEEE Transactions on Power Electronics*, vol. 32, no. 7, pp. 5497-5508, (2017).

- [7] W. Ma, L. Wang, R. Zhang, J. Li, Z. Dong et al, "Hopf Bifurcation and Its Control in the One-Cycle Controlled Cuk Converter," *IEEE Transactions on Circuits and Systems II: Express Briefs*, vol. 66, no. 8, pp. 1411-1415, (2019).
- [8] B. R. Ananthapadmanabha, R. Maurya and S. R. Arya, "Improved Power Quality Switched Inductor Cuk Converter for Battery Charging Applications," *IEEE Transactions on Power Electronics*, vol. 33, no. 11, pp. 9412-9423, (2018).
- [9] A. Lekić, D. Stipanović and N. Petrović, "Controlling the Ćuk Converter Using Polytopic Lyapunov Functions," *IEEE Transactions on Circuits and Systems II: Express Briefs*, vol. 65, no. 11, pp. 1678-1682, (2018).
- [10] M. Khodabandeh, E. Afshari and M. Amirabadi, "A Family of Ćuk, Zeta, and SEPIC Based Soft-Switching DC–DC Converters," *IEEE Transactions on Power Electronics*, vol. 34, no. 10, pp. 9503-9519, (2019).
- [11] J. C. d. S. de Morais, J. L. d. S. de Morais and R. Gules, "Photovoltaic AC Module Based on a Cuk Converter With a Switched-Inductor Structure," *IEEE Transactions on Industrial Electronics*, vol. 66, no. 5, pp. 3881-3890, (2019).
- [12] A. K. Singh, A. K. Mishra, K. K. Gupta, P. Bhatnagar and T. Kim, "An Integrated Converter With Reduced Components for Electric Vehicles Utilizing Solar and Grid Power Sources," *IEEE Transactions on Transportation Electrification*, vol. 6, no. 2, pp. 439-452, (2020).
- [13] S. A. Ansari and J. S. Moghani, "A Novel High Voltage Gain Noncoupled Inductor SEPIC Converter," *IEEE Transactions on Industrial Electronics*, vol. 66, no. 9, pp. 7099-7108, (2019).
- [14] S. Lee and H. Do, "Isolated SEPIC DC–DC Converter with Ripple-Free Input Current and Lossless Snubber," *IEEE Transactions on Industrial Electronics*, vol. 65, no. 2, pp. 1254-1262, (2018).
- [15] H. Komurcugil, S. Biricik and N. Guler, "Indirect Sliding Mode Control for DC–DC SEPIC Converters," *IEEE Transactions on Industrial Informatics*, vol. 16, no. 6, pp. 4099-4108, (2020).